

Article citation info:

Lozia Z. Is the representation of transient states of tyres a matter of practical importance in the simulations of vehicle motion? The Archives of Automotive Engineering – Archiwum Motoryzacji. 2017; 77(3): 63-84, <http://dx.doi.org/10.14669/AM.VOL77.ART5>

IS THE REPRESENTATION OF TRANSIENT STATES OF TYRES A MATTER OF PRACTICAL IMPORTANCE IN THE SIMULATIONS OF VEHICLE MOTION?

CZY OPIS STANÓW NIEUSTALONYCH OGUMIENIA W SYMULACJI RUCHU POJAZDÓW MA ZNACZENIE PRAKTYCZNE?

ZBIGNIEW LOZIA¹

Warsaw University of Technology

Summary

There are quite few publications where the representation of transient states of tyres is taken into account in the examination of the motion of a vehicle as a whole by computer simulation. Most of the researchers who build models of motor vehicle dynamics leave this issue out of account, believing that it is related to the phenomena of little importance in both qualitative and quantitative terms, especially when self-excited vibration of wheels with pneumatic tyres is ignored.

The objective of this publication is to present simulations of motor vehicle motion in the situation encountered during the training of drivers at Driver Improvement Centres. The author proves that the taking into account of the representation of transient states of the lateral force and aligning moment on vehicle tyres will strongly affect the calculation results. This is because of the excitation form, the time constants of which are comparable with the relaxation time of the tyres of the vehicle under test. The analysis results have been presented in both quantitative and qualitative form, i.e. in a table and as time histories of selected quantities, respectively. The data shown indicate considerable differences in the calculated effects of disturbance to rectilinear motion of a passenger car, when

¹ Warsaw University of Technology, Faculty of Transport, ul. Koszykowa 75, 00-662 Warszawa, Poland; e-mail: lozia@wt.pw.edu.pl

determined with ignoring the transient states of tyres, in comparison with the corresponding calculation results obtained with the transient states of tyres having been taken into account. The biggest differences in the absolute values recorded during the first second from the beginning of the disturbance to the motion of rear vehicle wheels were observed in yaw (heading) angle, lateral displacement of the centre of vehicle mass, and moment of forces on the steering wheel. The differences were so big (from 19 % to 26 %) that they changed the qualitative and quantitative assessment of vehicle behaviour. Thus, they highlighted the great impact that the representation of transient states of the lateral forces and aligning moments on vehicle tyres exerts on the results of the test being simulated.

Keywords: wheel with a pneumatic tyre, tyre sideslip, transient state, relaxation, simulation

Streszczenie

Niewiele jest prac, w których uwzględnia się opis stanów nieustalonych ogumienia w badaniach symulacyjnych ruchu całego pojazdu. Większość osób budujących modele dynamiki samochodów pomija ten opis, uznając, że dotyczy zjawisk mało istotnych z jakościowego i ilościowego punktu widzenia, zwłaszcza wtedy, gdy pomijane są drgania samowzbudne kół ogumionych.

Celem niniejszej publikacji jest przedstawienie symulacji ruchu samochodu w sytuacji, która jest spotykana w trakcie treningów kierowców w Ośrodku Doskonalenia Techniki Jazdy. Autor udowadnia, że uwzględnienie opisu stanów nieustalonych siły bocznej i momentu stabilizującego ogumienia w bardzo istotny sposób wpływa na wyniki przeprowadzonych obliczeń. Wynika to z postaci wymuszenia, którego stałe czasowe są porównywalne z czasem nabiegania ogumienia badanego pojazdu. Autor przedstawia wyniki ilościowo w formie tabeli oraz jakościowo w postaci przebiegów czasowych wybranych wielkości. Wskazują one na istotne różnice między efektami zaburzenia ruchu prostoliniowego samochodu osobowego, dla przypadku nieuwzględniania stanów nieustalonych ogumienia, odniesionymi do wyników otrzymanych dla przypadku uwzględniania stanów nieustalonych ogumienia. Największe różnice modułów w trakcie pierwszej sekundy od wystąpienia zaburzenia ruchu kół osi tylnej, dotyczą kąta odchylenia (kąta kierunkowego), przemieszczenia poprzecznego środka masy pojazdu oraz momentu na kole kierownicy. Są one na tyle istotne (od 19 do 26%), że zmieniają jakościowo i ilościowo ocenę zachowania pojazdu. Wskazują, zatem, na duży wpływ opisu stanów nieustalonych sił bocznych i momentów stabilizujących kół jezdnych na wyniki symulowanego testu.

Słowa kluczowe: koło ogumione, boczne znoszenie, stan nieustalony, relaksacja, symulacja

1. Introduction

In real vehicles, transient states of tyre-road interaction are an element in the kinematic and dynamic properties of the vehicles. The transient states are always encountered when a rapid change takes place in tyre sideslip angle, circumferential tyre slip ratio, normal road reaction force, or camber angle. The effects of transient states of tyre-road interaction were described in [6, 7, 11, 12, 13, 14, 15, 17, 18, 19, 21, 22, 23, 24, 25, 26, 27, 28]. Such states are an important element in the analysis of self-excited vibration of airplane wheels [27] and steered wheels of motor vehicles [6], especially motorcycles [18, 24, 25, 28].

Most of the researchers who build simulation models of the motion or dynamics of motor vehicles leave the representation of such phenomena out of account, believing that they are of little importance in both qualitative and quantitative terms, especially when

self-excited vibration of wheels with pneumatic tyres is ignored. The works where the representation of transient states of tyres is taken into account in the examination of the motion of a vehicle as a whole make only a few exceptions [7, 13, 15, 18, 21, 22]. The results presented chiefly highlight the qualitative significance of these phenomena, while their quantitative role is considered less important (e.g. [7]).

The objective of this publication is to present simulations of motor vehicle motion in a situation corresponding to real conditions, where transient states of the sideslip of vehicle's pneumatic tyres play a role considered important in both qualitative and quantitative terms.

2. Transient states of tyre-road interaction

Rapid changes in the steering angle or braking torque (resulting from the operation of the ABS, ASR - TCS or the like systems) as well as road surface irregularities (having an impact on the normal road reaction force) cause changes in the following quantities that describe the state of tyre-road interaction: tyre sideslip angle, circumferential tyre slip ratio, normal road reaction force, and camber angle. The resulting "transient state of tyre-road interaction" is characterized by lateral force and aligning moment values different from the steady-state values of these parameters. Their absolute values decrease and a time delay appears between the "input" (e.g. tyre sideslip angle) and the "response" (lateral force and aligning moment). More precisely, the tyre must travel a certain distance (referred to as "relaxation length") to reach a load state (understood in general terms, not only as vertical load) corresponding to the steady-state load. Fig. 1 shows changes in lateral force B_p , acting on the tyre, in response to a step change in tyre sideslip angle δ . The wheel centre moves with a velocity of v ; B_{pss} is the steady-state value of the lateral force corresponding to the sideslip angle δ . The parameter denoted by t_n (referred to as "relaxation time") is the time after which the tangent to curve $B_p(t)$ at a point with an abscissa of $t = 0$ reaches the value of B_{pss} . The product of relaxation time t_n [s] and velocity v [m/s] represents the said "relaxation length", denoted by l_n [m].

$$l_n = t_n \cdot v \quad (1)$$

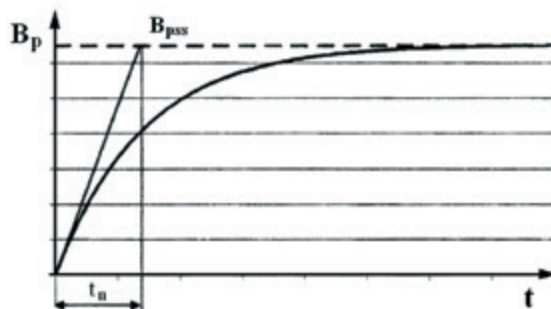


Fig. 1. Pneumatic tyre's response to a step change in tyre sideslip angle δ , i.e. changes in lateral force B_p as a function of time: B_{pss} – steady-state lateral force; t – time; t_n – relaxation time

For sinusoidal changes in the tyre sideslip angle, circumferential tyre slip ratio, normal road reaction force, or camber angle, the parameters of special importance are the amplitude and period of these changes, or rather their wavelength, thanks to which the input parameters (i.e. the period and wavelength) may be compared with the tyre relaxation length. Based on tyre tests carried out [17, 18, 24, 27, 28], a finding was formulated that transient states of tyres should be taken into account when the tyre relaxation length exceeds 0.1-0.25 (i.e. 10-25 %) of the shortest wavelength of the input (a specific value depends on the appropriate tyre-road interaction parameter). This is applicable, first of all, to inputs of periodical nature, e.g. caused by road irregularities or related to vibrations of steered wheels.

This article will present a description of motor vehicle motion formulated with taking into account transient tyre sideslip states, which induce transient states of the lateral forces and aligning moments on vehicle tyres.

3. Description of the transient values of the lateral force and aligning moment on the tyre

Fig. 2 depicts the quantities that describe the interaction between a pneumatic tyre and a horizontal road surface for the case of a pure tyre sideslip. Point U is a projection of the wheel centre onto the road surface. At point U_B , the resultant lateral force B_p is applied to the tyre. The product of force B_p and distance between points U_B and U is the tyre aligning moment. The $U\xi\eta$ coordinate system is a local system attached to the wheel. The $U\xi$ axis lies in the central plane of the wheel and in the road surface plane; v is a projection of the velocity of the centre of wheel onto the road surface; for the motion case under consideration, v is equal to the velocity of the centre of wheel and, simultaneously, to the vehicle velocity. The tyre sideslip angle has been denoted by δ . The positive senses of the quantities mentioned above are as shown in the drawing.

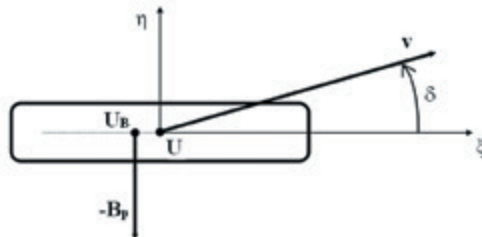


Fig. 2. The case of a pure sideslip of the pneumatic tyre. For the notation, see the text.

The interrelation between the quantities denoted as above has been described by the following differential equation, formulated in accordance with the Von Schlippe-Dietrich hypothesis ([27], taken from [17]):

$$\dot{B}_p + \frac{k_p}{c_p} \cdot v \cdot B_p = -k_p \cdot v \cdot \delta, \quad (2)$$

where k_p is lateral tyre stiffness [N/m] and c_p is the coefficient of resistance to tyre sideslip ("kinematic lateral stiffness", often referred to as "cornering stiffness") [N/rad].

This hypothesis was formulated in 1942 for aircraft tyres. In 1990s, the transient state of the lateral force was also described with the use of a first-order differential equation (e.g. in the "IPG-Tire" model [21, 22]), but written here in the following form:

$$t_n \cdot \dot{B}_p + B_p = B_{pss}, \quad (3)$$

where B_{pss} is the steady-state value [N] of the lateral force for the specific kinematic state of tyre-road interaction and t_n is the tyre "relaxation time" [s].

The authors of publications [21, 22] have not referred to publication [27], but it can be easily shown that equations (3) and (2) correspond with each other within the linear range of the model of the lateral force acting on the tyre. If both sides of equation (2) is divided by $v \cdot k_p / c_p$ then the result will be

$$\frac{c_p}{k_p \cdot v} \cdot \dot{B}_p + B_p = -c_p \cdot \delta \quad (4)$$

In [17, 27], the expression

$$\frac{c_p}{k_p} = l_n \quad (5)$$

is referred to as "relaxation length" of the tyre. This quantity is identical with that mentioned above where equation (1) has been described. It represents the distance that must be rolled by the tyre for the lateral force to build up to a predetermined value. For example: for the 165 R13 D124 tyre, $c_p \approx 34\,000$ N/rad; $k_p \approx 250\,000$ N/m; $l_n \approx 0.136$ m.

The ratio of tyre "relaxation length" l_n to velocity v defines the tyre "relaxation time" t_n .

$$t_n = \frac{l_n}{v} = \frac{c_p}{k_p \cdot v} \quad (6)$$

This quantity is also present in the first term of equation (3).

Let us note that for the linear range of the model of the lateral force acting on the tyre, the right side of equation (4) defines a positive value (i.e. a value consistent with the sense of the U_η axis) of lateral force B_p , which is equal to B_{pss} in the steady state. This sense of the axis (the positive sign of force B_p) corresponds to negative value of angle δ .

$$B_{pss} = -c_p \cdot \delta \quad (7)$$

As it can be seen from the above, equation (3) is fully equivalent to equation (2) (see also equations (4)-(7)). Hence, it is a simplified Von Schlippe-Dietrich equation. The authors of publications [21, 22] applied it to automotive tyres. They have indicated that for the objects of this type, the tyre "relaxation length" may be considered approximately equal to a half of the wheel circumference:

$$l_n = \pi \cdot r, \quad (8)$$

where r is the wheel radius [m].

For the 165 R13 D124 tyre, this value thus calculated is $l_n \approx 0.933$ m, i.e. it is about 7 times as long as that calculated from the original Von Schlippe-Dietrich theory. However, the analysis was carried out for a different object. The authors of publications [21, 22] have also reported that l_n noticeably depended on normal road reaction N . The tyre "relaxation length" l_n is declining with a decrease in the N value. Fig. 3 presents the "relaxation time" values t_n as a function of vehicle velocity $V = 3.6 \cdot v$ [km/h] for two forms of representation of the transient state of the lateral force: according to the simplified Von Schlippe-Dietrich hypothesis [7, 17, 27] and according to the IPG-Tire model [7, 21, 22].

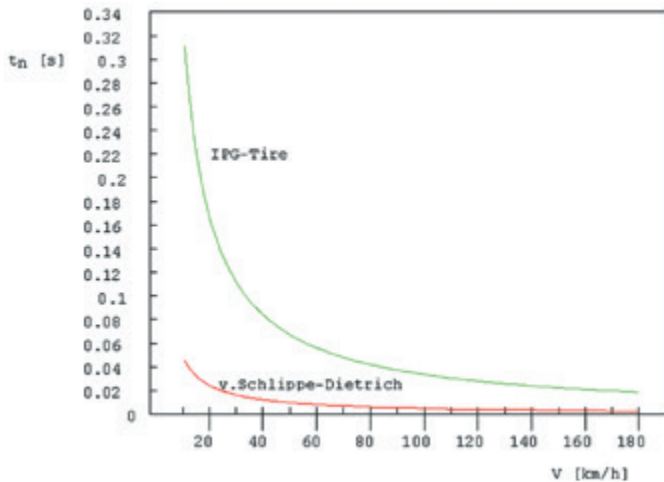


Fig. 3. "Relaxation time" vs. vehicle velocity for two estimations of the "relaxation length" for the 165 R13 D124 tyre, according to the simplified Von Schlippe-Dietrich hypothesis [7, 17, 27] and according to the IPG-Tire model [7, 21, 22]

When equations (5) and (7) are taken into account, equation (4) will take the form:

$$\dot{B}_p + \frac{V}{l_n} \cdot B_p = \frac{V}{l_n} \cdot B_{pss} \quad (9)$$

For constant velocity v and relaxation length l_n , the solution of differential equation (9) takes an analytical form convenient in numerical calculations for the time increment Δt adopted:

$$B_p(t) = B_{pss} - [B_{pss} - B_p(t - \Delta t)] \cdot \exp(-v \cdot \Delta t / l_n) \quad (10)$$

In one simulation step, the assumption that the velocity v and relaxation length l_n are constant is acceptable as it has not a considerable impact on the force $B_p(t)$ calculation accuracy.

To take into account the impact (noticed in the publications cited, e.g. [19, 25, 26, 11,12, 15]) of wheel load (normal road reaction) on the current value of tyre relaxation length l_n [m], the author has been adopting the following proportion in his programs [6, 7] since 1998:

$$\frac{l_n}{l_{nn}} = \frac{r_{sw} - r_d}{r_{sw} - r_{dn}} \quad (11)$$

and

$$l_{nn} = \pi \cdot r_{dn}, \quad (12)$$

where r_{dn} [m] is the "nominal" value of the dynamic tyre radius, corresponding to the vertical tyre load; l_{nn} [m] is the nominal value of the tyre relaxation length; r_{sw} [m] is the free tyre radius; and r_d [m] is the current value of the dynamic tyre radius, corresponding to the current vertical tyre load (normal road reaction).

Assuming the following empirical equation:

$$r_{dn} \approx 0.92 \cdot r_{sw}, \quad (13)$$

we obtain, after transformations:

$$l_n \approx 11.5 \cdot \pi \cdot (r_{sw} - r_d) = 36.128 \cdot (r_{sw} - r_d) \quad (14)$$

Fig. 4 shows the result of using the IPG-Tire model for the Michelin 195/65R15 tyre. This is a solution of differential equation (9), where changes in transient-state lateral force B_{pn} are represented as an effect of a step change in the tyre sideslip angle to a value of $\delta = 0.05$ rad ("Del" in the graphs). The single-step analytical form (10) was used, with the time increment having been adopted as $\Delta t = 0.001$ s. The wheel centre velocity was $V = 50$ km/h = 13.89 m/s = v , normal road reaction was $Z = 4\,800$ N, cornering stiffness was $c_p = 68\,000$ N/rad, free tyre radius was $r_{sw} = 0.316$ m, and dynamic tyre radius was $r_d = 0.296$ m. Relaxation time t_n is interpreted in physical terms as the time after which the tangent to curve $B_p(t)$ according to (1) (in this case denoted by $B_{pn}(t)$) reaches the value of B_{pss} , i.e. the steady-state value of the lateral force. Actually, the B_{pn} value is then equal to about 63 % of B_{pss} .

Fig. 5 shows a time history of the transient-state lateral force B_{pn} as an effect of three step changes in the sideslip angle to $\delta = \text{Del} = \pm 0.05$ rad in succession for the Michelin

195/65R15 tyre. The description of the test parameters corresponds to that concerning the case illustrated in Fig. 4. It can be clearly seen that lateral force B_{pn} is delayed in relation to sideslip angle $\delta = \text{Del}$. After the disappearance of the sideslip angle (for $t > 0.45$ s), lateral force B_{pn} maintains its non-zero value for a time longer than 0.3 s. Such an effect is not revealed in the case where lateral force B_{pss} is described with the transient state being ignored.

The transient state of the lateral force results in a transient value of the aligning moment, too. This is an effect of non-uniform distribution of the lateral force in the tyre-road contact patch. The resultant lateral force is shifted rearwards by a distance of UU_B in relation to centre U of the contact patch (Fig. 2).

With reference to the conclusion presented in item 2, a statement should be made that the relations between the parameters of change in the input and the tyre relaxation length remain important if the analysis is limited to the transient states of the lateral force and aligning moment caused by rapid changes in the sideslip angle. According to [28]: if the wavelength of changes in sideslip angle δ is of the same order as, or shorter than, tyre relaxation length l_n , then the transient states have a significant impact on the lateral force. If the wavelength of changes in δ is at least 8–10 times as long as l_n , then quasi-static tyre characteristics may be adopted.

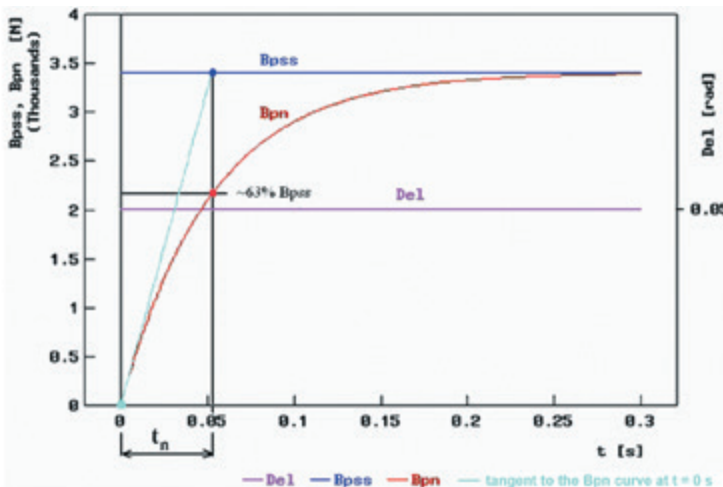


Fig. 4. Model IPG-Tire. Time history of transient-state lateral force B_{pn} as an effect of a step change in the tyre sideslip angle to a value of $\text{Del} = 0.05$ rad. B_{pss} is the value of the steady-state lateral force. Normal road reaction: $Z = 4\,800$ N; wheel centre velocity: $V^{pss} = 50$ km/h = 13.89 m/s = v ; time increment: $\Delta t = 0.001$ s; relaxation length: $l_n = 0.723$ m; relaxation time: $t_n = l_n/v = 0.052$ s. Tyre: Michelin 195/65R15

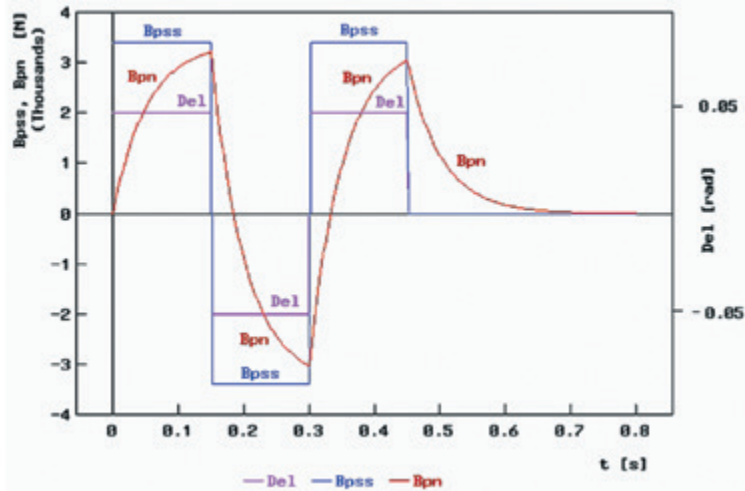


Fig. 5. Model IPG-Tire. Time history of transient-state lateral force B_{pn} as an effect of three step changes in the sideslip angle to $\delta = \text{Del} = \pm 0.05$ rad in succession. B_{pss} is the value of the steady-state lateral force. Normal road reaction: $Z = 4\,800$ N; wheel centre velocity: $V = 50$ km/h = 13.89 m/s = v ; time increment: $\Delta t = 0.001$ s; relaxation length: $l_n = 0.723$ m; relaxation time: $t_n = l_n/v = 0.052$ s. Tyre: Michelin 195/65R15

4. Simulated vehicle motion test where the significant importance of transient states of the lateral force and aligning moment on vehicle tyres has become apparent

This work was done with utilizing author's experience in the simulation of tests carried out at Driver Improvement Centres (DIC), where the motion of a vehicle under test was disturbed before the vehicle entered a skid pad, i.e. an area with reduced tyre-to-road adhesion [9, 10], by means of a dynamic "kick plate" (Fig. 6). Such a kick plate must be available at every Centre of this kind, according to the Regulation of the Polish Minister of Transport, Construction and Maritime Economy of 16 January 2013 on the improving of driving techniques [20]. In practice, the said disturbance is induced in most cases by causing a lateral displacement (jerk) of the kick plate (relative to the vehicle path) at the instant when the wheels of one vehicle axle have just left the kick plate and the wheels of the other vehicle axle are still moving on it. The disturbance caused by such a movement of the plate forces the driver to undertake defensive manoeuvres.



Fig. 6. Rectangular skid pad (the bright area) with a kick plate (the black tetragon), manufactured in Poland by UNIMETAL Sp. z o.o. of Złotów [29]

Fig. 7 shows a projection of the contour of the motor vehicle under test against the background of the kick plate [9, 10] and a physical model of a passenger car with the coordinate systems adopted [8, 9]. The length and width of the moving part of the kick plate are l_p [m] and s_p [m], respectively. These drawings were used as a basis for modifications to the model and program for the simulation of motion of the vehicle on the test track on which the drivers examined are tested [8, 9, 10].

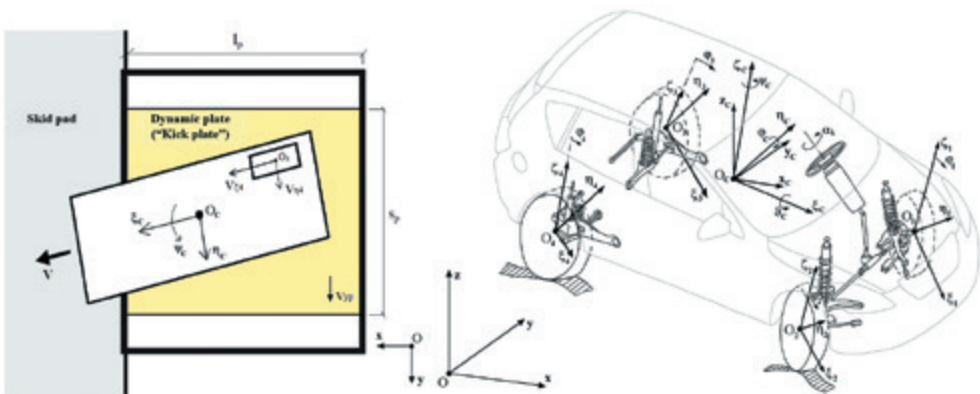


Fig. 7. Projection of the contour of the motor vehicle under test against the background of the kick plate (the positive senses of the quantities represented are as shown) [9, 10] and a physical model of a passenger car (two-axle vehicle with independent front and rear wheel suspension systems) together with the coordinate systems adopted [8, 9]

The model of a two-axle passenger car shown in Fig. 7 consists of nine mass elements: vehicle body solid (treated as a rigid body), four material particles O_1 , O_2 , O_3 , and O_4 , where the vehicle "unsprung masses" have been concentrated (including road wheels in their

translational motion), and four solids representing the rotating road wheels (exclusively in their rotational motion) [6, 8].

The following coordinate systems have been adopted [4, 5, 6, 8, 9, 10, 16]:

- O_{xyz} – an inertial system, fixed to the road, with the O_x and O_y axes being horizontal and the vertical axis O_z pointing upwards;
- $O_C x_C y_C z_C$ – a non-inertial system, with its axes being respectively parallel to axes O_x , O_y , and O_z and with its origin situated at the centre of mass of the vehicle body solid O_C ;
- coordinate systems fixed to the rigid bodies of the model, i.e. body solid ($O_C \xi_C \eta_C \zeta_C$) and four road wheels ($O_1 \xi_1 \eta_1 \zeta_1$, $O_2 \xi_2 \eta_2 \zeta_2$, $O_3 \xi_3 \eta_3 \zeta_3$, $O_4 \xi_4 \eta_4 \zeta_4$);
- auxiliary systems, facilitating the defining of transformation matrices.

To describe the translational motion of the solids and material particles of the model, the positions of the centres of mass (O_C , O_1 , O_2 , O_3 , O_4) of the said solids are used. The axes $O_i \xi_i$, $O_i \eta_i$, $O_i \zeta_i$ ($i = C, 1, 2, 3, 4$) are treated as the principal central axes of inertia of the corresponding rigid bodies. The rotation of the vehicle body solid about the fixed point O_C has been described with the use of "aircraft angles", also referred to as "quasi-Euler angles" [4, 5, 6, 8, 9, 10, 16]. The axes of individual rotations are treated as the principal central axes of rotation of the vehicle body solid.

The actual characteristics of the steering angles have been implemented as functions of the steering wheel angle α_k for the system without load. The flexibility of the steering system have been also taken into account. Additional steering angles have been introduced as functions of the aligning moments, torsional flexibility of the steering column with the steering gear, and flexibility of the left and right side of the steering linkage [6, 8, 9, 10]. The tyre-road contact forces have been described with the use of the HSRI-UMTRI model [2, 3] supplemented with a representation of the aligning moment and the IPG Tire model of transient states of tyres [21, 22]. To represent the forces developing within the tyre-road contact patch, the spring characteristics of the pneumatic tyre have also been taken into account [6, 8, 9, 10].

The equations of motion have been derived with the use of Lagrange equations of the second kind (e.g. [4, 5]). Prior to this, the following 14 generalized coordinates were adopted:

$q_1 = x_{OC}$, $q_2 = y_{OC}$, $q_3 = z_{OC}$ – coordinates defining the position of the centre of mass of the vehicle body solid (O_C) in the inertial reference system O_{xyz} ;

$q_4 = \psi_C$, $q_5 = \varphi_C$, $q_6 = \vartheta_C$ – coordinates describing the rotation of the vehicle body solid about its centre of mass O_C ; these are the quasi-Euler (aircraft) angles, i.e. heading (yaw) angle, pitch angle, and bank (roll) angle, respectively;

$q_7 = \zeta_{CO1}$, $q_8 = \zeta_{CO2}$, $q_9 = \zeta_{CO3}$, $q_{10} = \zeta_{CO4}$ – coordinates describing the motion of points O_1 , O_2 , O_3 , O_4 relative to the vehicle body solid in the direction of axis $O_C \zeta_C$ of the $O_C \xi_C \eta_C \zeta_C$ coordinate system; to these points, the "unsprung masses" of the suspension system are reduced;

$q_{11} = \varphi_1$, $q_{12} = \varphi_2$, $q_{13} = \varphi_3$, $q_{14} = \varphi_4$ – angles of rotation of road wheels (front left and right and rear left and right wheel, respectively).

A more detailed description of the family of models of motion and dynamics of two-axle vehicles and a description of the tyre-road interaction may be found in reference literature items [6, 7, 8, 9, 10] published by the author of this study.

The vehicle data correspond to the nominal specifications of the Kia cee'd SW car in running order, loaded with a driver and a driving instructor. The vehicle has a front-engine, front-wheel-drive layout. The total mass of the vehicle under test was 1570 kg, wheelbase was $l = 2.655$ m, distances between the centre of mass and the front and rear axle planes were $l_1 = 0.976$ m and $l_2 = 1.679$ m, respectively, static height of the centre of sprung mass was $z_{Oc} = 0.516$ m, and static height of the centre of vehicle mass was 0.501 m. The vehicle moved with a velocity of $V = 50$ km/h = 13.89 m/s = v .

The kick plate (Fig. 6) parameters were assumed in accordance with the specifications of the prototype facility modernized in 2016 and manufactured by a Polish company UNIMETAL [29], i.e. length $l_p = 3.0$ m, width $s_p = 2.7$ m, and extreme lateral displacement $s_{yp} = 0.3$ m. The maximum velocity and acceleration of the kick plate displacement was $v_{ypmax} = 1.5$ m/s and $[d(v_{yp})/dt]_{max} = 15$ m²/s, respectively. The plate was coated with a material for which the maximum value of the coefficient of adhesion was 0.8. The author interprets this figure as the value of the coefficient of adhesion for a tyre slip velocity close to zero. For the skid pad, the maximum value of the coefficient of adhesion was assumed as 0.5. The road, skid pad, and kick plate surfaces were assumed as being horizontal and even.

Fig. 8 shows the assumed form of the instantaneous (current) kick plate velocity v_{ypa} [m/s] as a function of time t . TPL1 [s] and TPL2 [s] represent the instants when the kick plate starts moving and stops, respectively. TYPL [s] is the total time of lateral displacement of the kick plate. TPLKN [s] is the time during which the lateral velocity of the kick plate grows from zero to a constant value v_{ypmax} [m/s]. TPLKS is the time during which the lateral velocity of the kick plate drops from the constant value v_{ypmax} [m/s] to zero. TKTPL [s] is the time of the rear vehicle wheels being present on the kick plate, for the rectilinear motion along the kick plate symmetry plane.

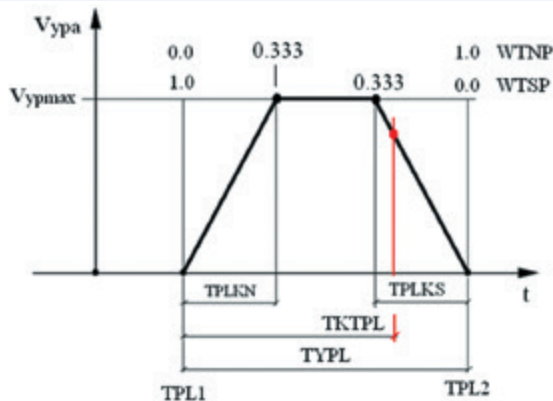


Fig. 8. Assumed form of the current kick plate velocity v_{ypa} as a function of time t , for constant values of $WTNP = TPLKN / TYPL$ and $WTSP = TPLKS / TYPL$ and for $TYPL = \text{const}$. $TKTPL$ [s] is the time of the rear vehicle wheels being present on the kick plate

The kick plate motion parameters presented may be calculated as shown below (see also Fig. 8). The time of the rear vehicle wheels being present on the kick plate, for the rectilinear motion along the kick plate symmetry plane, was:

$$TKTPL = l_p/v = 3.0 \text{ m}/13.89 \text{ m/s} = 0.216 \text{ s} \quad (15)$$

The time of growth and drop in the lateral velocity of the kick plate was:

$$TPLKN = TPLKS = v_{ypmax}/[d(v_{yp})/dt]_{max} = 1.5 \text{ m/s} / 15 \text{ m/s}^2 = 0.1 \text{ s} \quad (16)$$

The total time of lateral displacement of the kick plate was:

$$TYPL = s_{yp}/v_{ypmax} + 0.5 \cdot (TPLKN + TPLKS) = 0.3 \text{ m} / 1.5 \text{ m/s} + 0.5 \cdot (0.1 \text{ s} + 0.1 \text{ s}) = 0.3 \text{ s} \quad (17)$$

The values of the dimensionless coefficients defining the intervals of growth and drop in the lateral kick plate velocity v_{yps} [m/s] were:

$$WTNP = TPLKN / TYPL = 0.1 \text{ s} / 0.3 \text{ s} = 0.333 \quad (18)$$

$$WTSP = TPLKS / TYPL = 0.1 \text{ s} / 0.3 \text{ s} = 0.333 \quad (19)$$

5. Simulation results in the form of time histories of selected quantities

The driver senses a disturbance to vehicle motion through, above all, the following quantities:

- lateral vehicle acceleration a_{nh} ("aetah" in the graphs) and vehicle yaw velocity $d\psi_c/dt$ ("psiCp" in the graphs); these define the force of inertia acting on driver's body and detected by the balance organs in driver's inner ear and by sensory receptors in his/her limbs and trunk;
- lateral displacement of the centre of vehicle mass y_{oc} ("yOC" in the graphs) and vehicle yaw (heading) angle ψ_c ("psiC" in the graphs), detected by the sense of sight;
- moment of forces on the steering wheel EMK, detected by hands (more precisely: by sensory receptors in the upper limbs).

It is the time histories and extremums of these quantities that have a decisive impact on driver's reactions. In addition to this, the time histories of tyre sideslip angles $\delta(i)$ ("Del(i)" in the graphs) and lateral forces ("Bp(i)" in the graphs) at individual tyres (identified by indicator "i") are important from the vehicle dynamics point of view. The time value $t = 0$ has been assumed to represent the instant when the kick plate started moving.

The simulation results were assessed with taking into account, first of all, the values taken by the quantities under analysis during the first second from the beginning of the disturbance to vehicle motion. This is a consequence of an assumption made that during the typical driver reaction time, estimated at 1 s [1], the driver is unable to undertake any action (i.e. to operate any of the vehicle controls) that might change the state of vehicle motion. The driver's reactions can only affect the vehicle motion during the next seconds (not covered by the scope of the simulation tests reported herein), and only those reactions may be taken as a basis to assess the driver at the examination or training carried out.

Fig. 9 shows the lateral displacement of the centre of vehicle mass y_{OC} as a function of time, determined for the model with and without a representation of transient states of vehicle tyres. Noteworthy are big qualitative and quantitative differences in the results obtained. At the end of the test, the values of the lateral vehicle displacement differed from each other by more than 5 m.

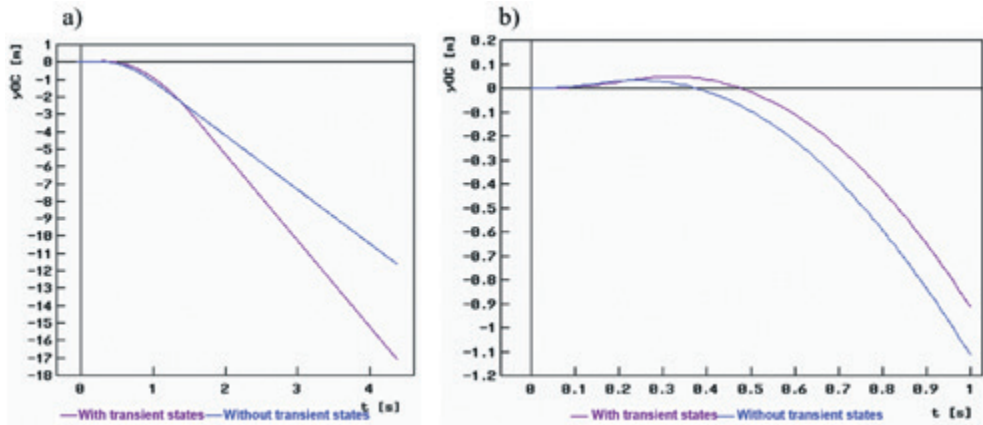


Fig. 9. Lateral displacement of the centre of vehicle mass vs. time. Two-axle passenger car, disturbance applied to rear vehicle wheels, test results obtained for a model with and without a representation of transient states of vehicle tyres, $V = 50 \text{ km/h} = 13.89 \text{ m/s}$: a) full range of the parameters simulated; b) one-second fragment

Fig. 10 shows a comparison of the results defining the vehicle yaw angle. The taking of transient states of vehicle tyres into account results in very big differences in the angular vehicle position as early as during the first second from the beginning of the disturbance to vehicle motion.

Fig. 11 shows the vehicle yaw velocity as a function of time. These graphs are a consequence of the results that can be seen in the preceding figure, as they visualize the derivative of the vehicle yaw angle. The differences in the curves are significant, too.

The lateral acceleration of the centre of vehicle mass in a system reduced to the horizontal plane has been presented as a function of time in Fig. 12. The extreme values are close to each other. Attention is attracted by a time shift and a long period of non-zero acceleration values obtained for the model where transient states of vehicle tyres are taken into account.

The lateral forces on the front and rear axle wheels have been illustrated in Figs. 13 and 14, respectively. Considerable differences can be seen in the results obtained for the models where transient states of vehicle tyres were and were not represented. The curves plotted for the case with the transient states being taken into account show much longer periods of the lateral forces differing from zero. The non-zero lateral forces were also the main reason for the fact that the results that can be seen in Fig. 12 were as presented.

Figs. 15 and 16 show one-second fragments, plotted for time interval $\langle 0 \text{ s}, 1 \text{ s} \rangle$, of the time histories of the lateral forces on the front and rear axle wheels as presented in Figs. 13 and 14.

Thanks to the graph extension effect thus produced, a significant time delay can be clearly seen in the force curves obtained with taking into account transient states of vehicle tyres in comparison with the curves where the transient states have not been represented.

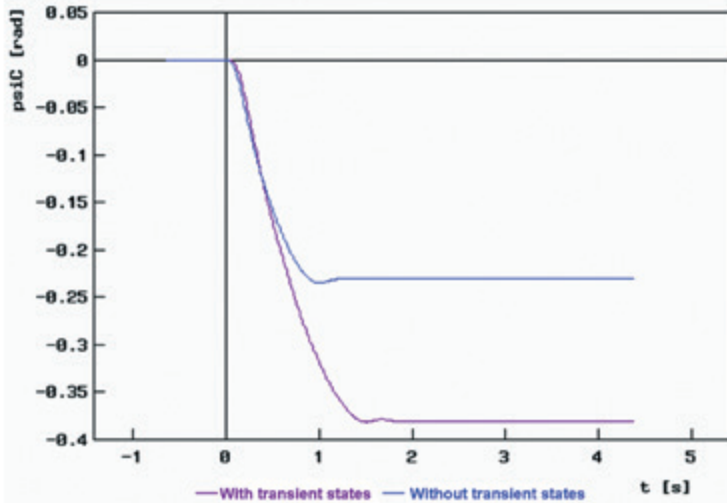


Fig. 10. Vehicle yaw angle vs. time. Two-axle passenger car, disturbance applied to rear vehicle wheels, test results obtained for a model with and without a representation of transient states of vehicle tyres, $V = 50 \text{ km/h} = 13.89 \text{ m/s}$

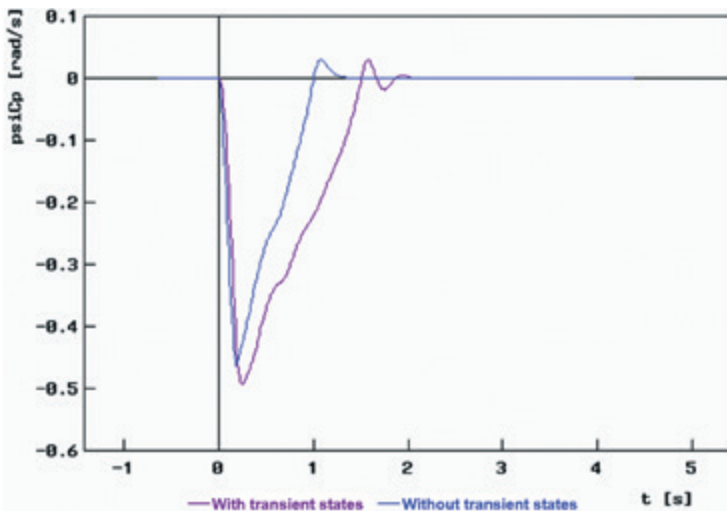


Fig. 11. Vehicle yaw velocity vs. time. Two-axle passenger car, disturbance applied to rear vehicle wheels, test results obtained for a model with and without a representation of transient states of vehicle tyres, $V = 50 \text{ km/h} = 13.89 \text{ m/s}$

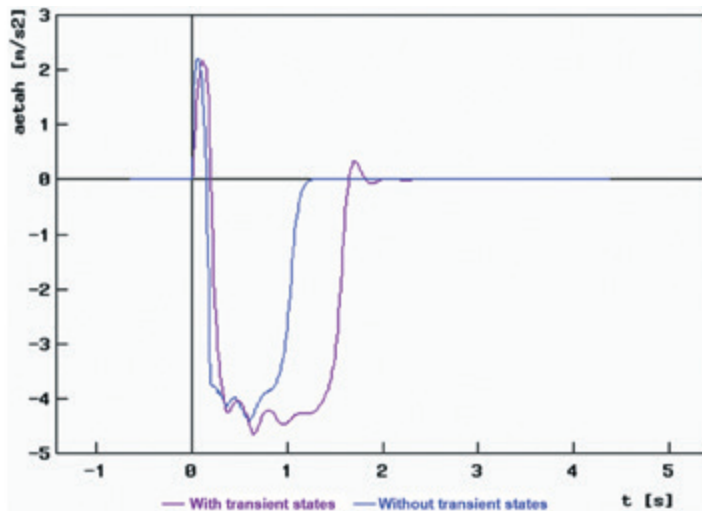


Fig. 12. Time histories of the lateral acceleration of the centre of vehicle mass in a system reduced to the horizontal plane. Two-axle passenger car, disturbance applied to rear vehicle wheels, test results obtained for a model with and without a representation of transient states of vehicle tyres, $V = 50 \text{ km/h} = 13.89 \text{ m/s}$

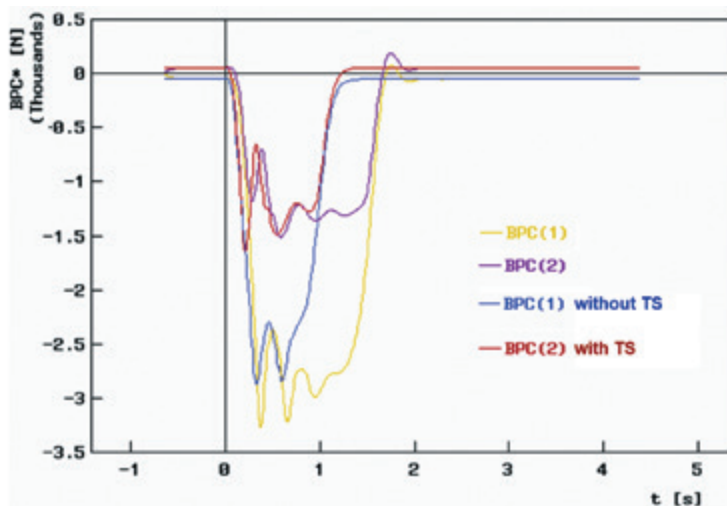


Fig. 13. Lateral forces on the front axle wheels vs. time: (1) – front left wheel; (2) – front right wheel. Two-axle passenger car, disturbance applied to rear vehicle wheels, test results obtained for a model with and without a representation of transient states of vehicle tyres ("without TS"), $V = 50 \text{ km/h} = 13.89 \text{ m/s}$

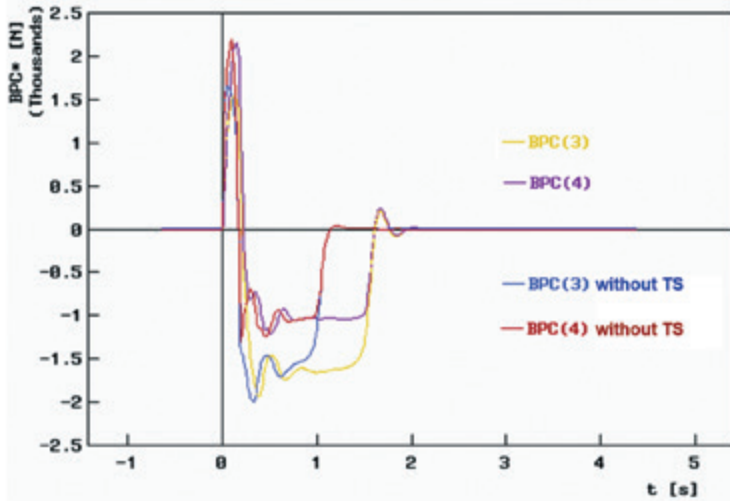


Fig. 14. Lateral forces on rear axle wheels vs. time: (3) – rear left wheel; (4) – rear right wheel. Two-axle passenger car, disturbance applied to rear vehicle wheels, test results obtained for a model with and without a representation of transient states of vehicle tyres ("without TS"), $V = 50 \text{ km/h} = 13.89 \text{ m/s}$

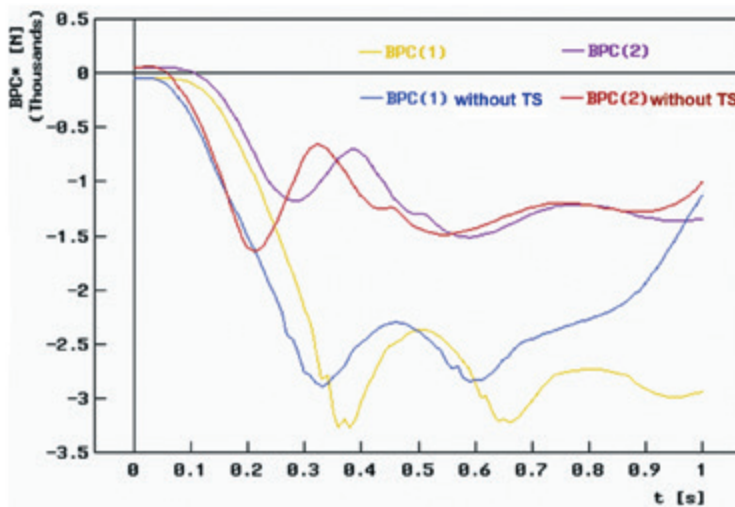


Fig. 15. Fragment of Fig. 13 for time interval $(0 \text{ s}, 1 \text{ s})$. Lateral forces on the front axle wheels vs. time: (1) – front left wheel; (2) – front right wheel. Disturbance applied to rear vehicle wheels, test results obtained for a model with and without a representation of transient states of vehicle tyres ("without TS"), $V = 50 \text{ km/h} = 13.89 \text{ m/s}$

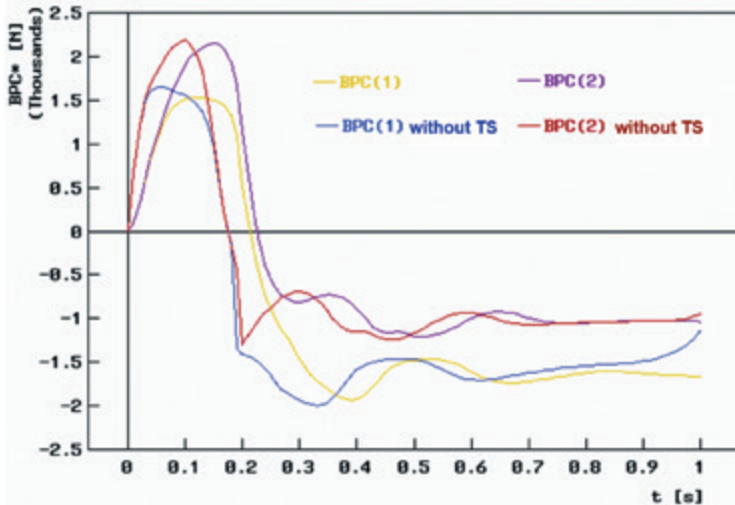


Fig. 16. Fragment of Fig. 14 for time interval (0 s, 1 s). Lateral forces on rear axle wheels vs. time: (3) – rear left wheel; (4) – rear right wheel. Disturbance applied to rear vehicle wheels, test results obtained for a model with and without a representation of transient states of vehicle tyres ("without TS"), $V = 50 \text{ km/h} = 13.89 \text{ m/s}$

6. Recapitulation of simulation calculation results

The simulation results presented above in the graphic form will be tabulated, recapitulated, and interpreted below.

As previously mentioned, the driver senses a disturbance to vehicle motion chiefly through changes in the lateral acceleration and yaw velocity of the vehicle, in the lateral displacement of the centre of vehicle mass and vehicle yaw (heading) angle, and in the moment of forces on the steering wheel. It is the time histories and extremums of these quantities that have a decisive impact on driver's reactions.

The quantitative assessment of simulation results was done with taking into account absolute values of the quantities under analysis that were recorded during the first second from the beginning of the disturbance. This is a consequence of an assumption made that during the typical driver reaction time, estimated at 1 s [1], the driver is unable to undertake any action. Table 1 shows a summary of results of the simulation of motion of a two-axle passenger car for the case that transient states of vehicle tyres were ignored in comparison with the case that transient states of vehicle tyres were taken into account in accordance with the IPG-Tire model.

Table 1. Summary of results of the simulation of motion of a two-axle passenger car for the case that transient states of vehicle tyres were ignored in comparison with the case that transient states of vehicle tyres were taken into account in accordance with the IPG-Tire model. Two-axle passenger car, disturbance applied to rear vehicle wheels, $V = 50 \text{ km/h} = 13.89 \text{ m/s}$

Criterion for the time interval (0 s, 1 s) from the start of kick plate's motion	Model of transient states of tyres: IPG-Tire	Model of transient states of tyres: inactive	Change in the absolute value of the quantity assessed in comparison with that obtained for the active model of transient states
Extremum of the lateral displacement of the centre of vehicle mass y_{oc} [m]	-0.911	-1.112	+22.1 %
Extremum of the yaw angle of the vehicle body solid psiC [rad]	-0.31778	-0.23501	-26.0 %
Extremum of the yaw velocity of the vehicle body solid psiCp [rad/s]	-0.49263	-0.46367	-5.9 %
Extremum of the lateral acceleration of the centre of vehicle mass a_{etah} [m/s ²]	-4.65	-4.41	-5.2 %
Extremum of the moment of forces on the steering wheel EMK [Nm]	10.13	12.10	+19.4 %

The results presented in quantitative terms in Table 1 and in qualitative terms in the form of time histories of selected quantities in Figs. 9-16 indicate considerable differences between the effects of disturbance to rectilinear motion of a passenger car, calculated with ignoring transient states of vehicle tyres, and the corresponding figures calculated for the transient states of vehicle tyres being taken into account. The biggest differences in the absolute values of the said quantities, which occurred during the first second from the beginning of the disturbance to the motion of rear axle wheels, were observed in the yaw (heading) angle ψ_c , lateral displacement of the centre of vehicle mass y_{oc} , and moment of forces on the steering wheel EMK. The differences were so big (from 19 % to 26 %) that they changed the qualitative and quantitative assessment of vehicle behaviour. Thus, they highlighted the great impact that the representation of transient states of the lateral forces and aligning moments on vehicle tyres exerts on the results of the test being simulated.

This conclusion is confirmed by the time histories of the selected quantities characterizing the simulated manoeuvre during the first second and, moreover, during the whole 5 s period covered by the simulation (Figs. 9-16).

Considerable differences were observed in the lateral displacement of the centre of vehicle mass y_{oc} (see Fig. 9 and Table 1). They reached the highest values, exceeding 5 m,

at the end of the manoeuvre. The biggest quantitative differences occurred in the yaw angle of the vehicle body solid ψ_{IC} (see Fig. 10 and Table 1). They were observed in the time interval from 1 s till the end of the test. This parameter has a strong impact on driver's perception of the vehicle behaviour. For the other quantities presented, the differences in their extreme values, recorded for the first second from the beginning of the disturbance to the motion of rear axle wheels, were not so big; however, considerable qualitative differences in these quantities can be seen. Fig. 11 shows time histories of the vehicle yaw velocity and Fig. 12 shows time histories of the lateral acceleration of the centre of vehicle mass in a system reduced to the horizontal plane. For the model where transient states of the lateral forces acting on vehicle tyres are taken into account, a time delay of both of these parameters can be seen. These quantities have also non-zero values for a period much longer than that observed when transient states of vehicle tyres are ignored. The differences visualized in Figs. 11 and 12 arose from different time histories of the sideslip angles and of the corresponding lateral forces (see Figs. 13-16), determined from the model where transient states of the lateral forces on vehicle tyres are taken into account in comparison with the similar results obtained from the model where this phenomenon is ignored. This is a case where the said time delay can be seen again in the results obtained with taking into account transient states of the lateral forces on vehicle tyres. The non-zero values of these quantities persist for a much longer time, too. It is advisable to compare these results in qualitative terms with the curves presented in Figs. 4 and 5. Figs. 15 and 16 show fragments of the lateral force vs. time curves of Figs. 13 and 14, limited to the first second from the beginning of the disturbance to the motion of rear vehicle wheels. Thanks to a different time scale, the time delays mentioned above are better visible. They may even be coarsely estimated at about 0.1 s.

In recapitulation, a statement should be made that for the simulated test of disturbance to vehicle motion in the situation that is often encountered during the training of drivers at Driver Improvement Centres, the taking into account of the representation of transient states of vehicle tyres will strongly affect the calculation results. This is because of the excitation form, the time constants of which are comparable with the relaxation time of the tyres of the vehicle under test.

Acknowledgements

This study was carried out within cooperation between the Faculty of Transport of the Warsaw University of Technology and UNIMETAL Sp. z o.o. of Złotów.

The simulation model of motion of a passenger car, used for the calculations, was developed within project No. 0 ROB 0011 01/ID/11/1 *Simulator of driving emergency service vehicles during typical and extreme actions*, related to the construction of such a simulator by the ETC-PZL AI Company in Warsaw.

The full text of the article is available in Polish online on the website <http://archiwummotoryzacji.pl>.

Tekst artykułu w polskiej wersji językowej dostępny jest na stronie <http://archiwummotoryzacji.pl>.

References

- [1] Arczyński S. *Mechanika ruchu samochodu (Mechanics of motion of a motor vehicle)*. WNT. Warszawa 1993.
- [2] Dugoff H, Fancher P S, Segel L. An Analysis of Tire Traction Properties and their Influence on Vehicle Dynamic Performance. SAE Paper 700377.
- [3] Fancher P S JR, Bareket Z. Including Roadway and Tread Factors in Semi-empirical Model of Truck Tyres. Supplement to VSD. 1993 (21): 92-107.
- [4] Gutowski R. *Mechanika analityczna (Analytic mechanics)*. PWN. Warszawa 1971.
- [5] Kamiński E, Pokorski J. *Teoria samochodu. Dynamika zawiesznień i układów napędowych pojazdów samochodowych (Automobile theory. Dynamics of suspension systems and powertrains of motor vehicles)*. WKŁ. Warszawa 1983.
- [6] Lozia Z. *Analiza ruchu samochodu dwuosioowego na tle modelowania jego dynamiki. Monografia (Analysis of biaxial car motion based upon dynamic models. A monograph)*. Prace Naukowe Politechniki Warszawskiej – Transport. Warszawa 1998; 41.
- [7] Lozia Z. Ocena roli stanów niestabilnych ogumienia w badaniach dynamiki poprzecznej samochodu (Evaluation of the role of transient states of tyres in the research on lateral dynamics of the motor vehicle). Proceedings of the 7th International Symposium of the Institute of Motor Vehicles of the Military University of Technology "Improvement on Construction and Methods of Operation of Motor Vehicles", Part II. Warszawa-Rynia 8 10 Dec. 1999: 358-366.
- [8] Lozia Z. Modele symulacyjne ruchu i dynamiki dwóch pojazdów uprzywilejowanych (Vehicle dynamics simulation models of two emergency vehicles). *Czasopismo Techniczne. Mechanika / Technical Transactions. Mechanics*. 2012 (109); 3-M: 19-34.
- [9] Lozia Z. Modelling and simulation of a disturbance to the motion of a motor vehicle entering a skid pad as used for tests at Driver Improvement Centres (Modelowanie i symulacja zakłócenia ruchu samochodu w trakcie wjazdu na płytę poślizgową stosowaną w ośrodkach doskonalenia techniki jazdy). *The Archives of Automotive Engineering – Archiwum Motoryzacji*. 2015 (69); 3: 87-103 (in English) / 173-188 (in Polish).
- [10] Lozia Z. Simulation testing of two ways of disturbing the motion of a motor vehicle entering a skid pad as used for tests at Driver Improvement Centres (Symulacyjna ocena dwóch sposobów zakłócania ruchu samochodu w trakcie wjazdu na płytę poślizgową stosowaną w ośrodkach doskonalenia techniki jazdy). *The Archives of Automotive Engineering – Archiwum Motoryzacji*. 2016 (72); 2: 111-125. Available from: <http://dx.doi.org/10.14669/AM.VOL72.ART.6>
- [11] Luty W. Analiza właściwości ogumienia samochodu ciężarowego w niestabilnym stanie znoszenia bocznego (Analysis of the properties of motor truck tyres in transient sideslip state). *Zeszyty Instytutu Pojazdów Politechniki Warszawskiej*. 2000; 3 (38).
- [12] Luty W. Analiza nabiegania ogumienia nowych konstrukcji podczas toczenia ze znoszeniem bocznym w quasi-statycznych warunkach ruchu. (Analysis of the relaxation of tyres of new construction when rolling with sideslip in quasi-static conditions of motion). In: *Analiza wpływu ogumienia nowych konstrukcji na bezpieczeństwo samochodu w ruchu krzywoliniowym (Analysis of the influence of tyres of new construction on the motor vehicle safety in curvilinear motion)*. Military University of Technology. Warszawa 2009; ISBN978-83-61486-21-3; 19-26.
- [13] Luty W. Niestabilne stany znoszenia bocznego ogumienia kół jezdnych w symulacji ruchu krzywoliniowego pojazdu (Tire transient properties in simulation of vehicle lateral dynamics in curvilinear motion). *Prace Naukowe Politechniki Warszawskiej – Transport. Oficyna Wydawnicza Politechniki Warszawskiej*. 2013; 98: 357-367.
- [14] Luty W. Badania eksperymentalne ogumienia w niestabilnych warunkach znoszenia bocznego (Experimental research on tyres in transient sideslip conditions). *The Archives of Automotive Engineering – Archiwum Motoryzacji*. 2014 (66); 4; 23-32 (in English) / 133-141 (in Polish).
- [15] Luty W. Influence of the tire relaxation on the simulation results of the vehicle lateral dynamics in aspect of the vehicle driving safety. *Journal of Kones Powertrain and Transport*. 2015 (22); 1.
- [16] Maryniak J. *Dynamiczna teoria obiektów ruchomych (Dynamic theory of movable objects)*. Politechnika Warszawska. Prace Naukowe. Mechanika (Warsaw University of Technology. Scientific Works. Mechanics). WPW. 1976; 32.

- [17] Mitschke M. Teoria samochodu. Dynamika samochodu (Automobile theory. Dynamics of motor vehicles). WKŁ Warszawa 1977: 85-88.
- [18] Pacejka H B. Tire and vehicle dynamics. SAE 2002. SAE ISBN 0768011264.
- [19] Rill G. First order tire dynamics. 3rd European Conference on Computational Mechanics Solids, Structures and Coupled Problems in Engineering C.A. Mota Soares et.al. (ed.) Lisbon, Portugal, 5-8 June 2006.
- [20] Rozporządzenie Ministra Transportu, Budownictwa i Gospodarki Morskiej z dnia 16 stycznia 2013 r. w sprawie doskonalenia techniki jazdy (Regulation of the Polish Minister of Transport, Construction and Maritime Economy of 16 January 2013 on the improving of driving techniques). Dz. U. of 18 Jan. 2013, item 91.
- [21] Schieschke R. The importance of tire dynamics in vehicle simulation. Paper presented at The Tire Society. 9th Annual Meeting and Conference on Tire Science and Technology. Akron, Ohio, USA. March 20-21, 1990.
- [22] Schieschke R, Hiemenz R. The relevance of tire dynamics in vehicle simulation. XXIII FISITA Congress, Torino, Italy. May 7-11, 1990.
- [23] Segel L. Force and moment response of pneumatic tires to lateral motion inputs. Transactions ASME. J. of Engineering for Industry. 1966; 88B.
- [24] Segel L, Wilson R. Requirements for describing the mechanics of tires used on single-track vehicles. Vehicle System Dynamics. 1975 (4); 2-3.
- [25] Uil R T. Non-lagging effect of motorcycle tyres. An experimental study with the Flat Plank Tyre Tester. Eindhoven University of Technology. Department of Mechanical Engineering. Dynamics and Control Technology Group. Report No. DCT 2006.046. Eindhoven, June 2006.
- [26] Vantsevich V, Gray J P. Relaxation length review and time constant analysis for agile tire dynamics control. Proceedings of the ASME 2015 International Design Engineering Technical Conferences & Computers and Information in Engineering Conference. IDETC/CIE 2015, August 2-5, 2015, Boston, Massachusetts, USA. Conference Paper DOI: 10.1115/DETC2015-46798.
- [27] Von Schlippe B, Dietrich R. Zur Mechanik des Luftreifens Zentrale für Wissenschaftliches. Berichtswesen der Luftfahrtforschung. Berlin 1942.
- [28] Takahashi T, Pacejka H B. Cornering on uneven roads. Supplement to Vehicle System Dynamics., 1988 (17).
- [29] <http://www.unimetal.pl/pl/diagnostyka/oferta/andere-gerate/plyta-dynamiczna/> (cited: 09 May 2015).